ELSEVIER

Journal of Structural Geology 29 (2007) 1185–1200

JOURNAL OF STRUCTURAL GEOLOGY

www.elsevier.com/locate/jsg

Some considerations on the kinematics of chevron folds

F. Bastida [a,*], J. Aller [a], N.C. Toimil [b], R.J. Lisle [b], N.C. Bobillo-Ares [c]

[a] *Departamento de Geología, Universidad de Oviedo, Jesús Arias de Velasco s/n, 33005 Oviedo, Spain*
[b] *School of Earth, Ocean and Planetary Sciences, Cardiff University, Cardiff, CF10 3YE, UK*
[c] *Departamento de Matemáticas, Universidad de Oviedo, 33007 Oviedo, Spain*

Received 31 August 2006; received in revised form 26 February 2007; accepted 5 March 2007
Available online 15 March 2007

Abstract

Geometrical modelling and field analysis of chevron folds suggest that these structures are a result of the combination of several kinematical mechanisms, whose magnitude and order of application vary within certain limits. A possible mechanism operating early in the fold growth is homogeneous layer shortening, whose contribution is restricted by the high competence contrast that the multilayers developing chevron folds usually exhibit. In the early stages of folding, when the curvature is small, equiareal tangential longitudinal strain (ETLS) is an essential mechanism, since the operation of parallel tangential longitudinal strain (PTLS) or flexural flow (FF) would give rise respectively to area changes or strain in the limbs of the final fold that are too high to be geologically realistic. After folding by ETLS, probable mechanisms are PTLS and FF, which can operate in this order or simultaneously. In general, FF is necessary at the last stage of buckling, although the increment of folding due to this mechanism can be very small. High values of slip between layers and area change produced in the later stages of chevron folding can bring an end to buckling, probably at an interlimb angle value of 60–70°, and induce the onset of homogeneous strain (HS). This strain is not coaxial in many cases, with simple shear playing an important role, and gives rise to asymmetrical folds.

Keywords: Structural geology; Chevron folds; Folding mechanisms; Mathematical modelling

1. Introduction

Chevron folds can be defined as symmetric or slightly asymmetric angular folds that usually show an acute interlimb angle (Fig. 1). They are common in multilayers of alternating competent and incompetent rocks and their geometry, kinematics and mechanics have been studied by many authors (de Sitter, 1956, 1958; Bayly, 1964, 1976; Ramsay, 1967, 1974; Ghosh, 1968; Chapple, 1969, 1970; Johnson, 1970; Smythe, 1971; Johnson and Honea, 1975; Dubey and Cobbold, 1977; Casey and Huggenberger, 1985; Narahara and Wiltschko, 1986; Johnson and Pfaff, 1989; Pfaff and Johnson, 1989; Tanner, 1989; Stewart and Alvarez, 1991; Fowler and Winsor, 1996; Fletcher and Pollard, 1999; Pollard and Fletcher, 2005; among others).

Geometrical-kinematical studies (de Sitter, 1956, 1958; Ramsay, 1967, 1974; Ramsay and Huber, 1987; Pollard and Fletcher, 2005) are based on theoretical models that take into account the peculiarities of natural chevron folds and permit predictions to be made about the strain and displacements undergone by the folded rocks as well as the minor structures that can develop associated with this type of fold. Among the conclusions obtained in these studies are:

- When the multilayer is made up of competent layers, the development of chevron folds involves rotation of the limbs with associated slip between layers (de Sitter, 1956, 1958; Ramsay, 1967; Pollard and Fletcher, 2005). When chevron folds occur in sequences with alternating competent and incompetent beds, the slip between layers

* Corresponding author. Fax: +34 98 510 3103.
E-mail address: bastida@geol.uniovi.es (F. Bastida).

0191-8141/$ - see front matter © 2007 Elsevier Ltd. All rights reserved.
doi:10.1016/j.jsg.2007.03.010

Fig. 1. Chevron fold in Carboniferous greywacke and shale (Millook Haven, Cornwall, SE England).

is substituted by simple shear in the incompetent layers (Ramsay, 1974; Ramsay and Huber, 1987).

- The de Sitter (1956, 1958) and Pollard and Fletcher (2005) models do not describe the strain in the hinge zone, whereas in the Ramsay models (1967, 1974) the strain inside the competent layers is due to displacements parallel to the layer boundaries, that is, simple shear (flexural flow), and it involves no strain at the hinge points and maximum strain in the limbs.
- Ramsay (1967, 1974) deduces a geometric evolution of chevron folds using his models; this evolution involves that the fold maintains its chevron shape from the beginning of folding. De Sitter (1956, 1958) predicts a tightening of the chevron folds up to an interlimb angle of 50–60° at which the fold evolution stops.
- The De Sitter (1956, 1958) and Ramsay (1967, 1974) models predict the development of structures to accommodate the shape of the folded layers (bulbous hinges, boudinage, faults, hinge collapses, saddle reefs, etc.).

Mechanical studies have attempted to find the causes for the development of the angular form. Most of the explanations to this question are related to the well known concept of the plastic hinge (e.g. Johnson, 1970, pp. 301–304). In general they suggest that the angular form is linked to some type of non-linear rheological behaviour in the rocks during folding (Chapple, 1969, 1970; Lan and Hudleston, 1996), since the buckling theories involving linear behaviour predict sinusoidal or even more rounded forms for finite amplitudes (Ramberg, 1960; Biot, 1961, 1965; Biot et al., 1961; Currie et al., 1962; Chapple, 1968; Dieterich and Carter, 1969; Dieterich, 1970; Johnson and Fletcher, 1994; among others). This explanation has important kinematical implications, since it requires concentration of strain in a rounded hinge zone prior to the development of the angular form. Mechanical interaction between beds during folding can influence the development of chevron folds, as stated by Johnson and Honea (1975), who suggested that the core of concentric folds can be a favoured site for the nucleation of chevron folds.

Experimental models giving rise to chevron folds have provided insight into some aspects of the evolution of these folds and checking of some theoretical predictions. By these methods it is clearly confirmed that most chevron folds evolve from rounded folds and are produced first in their cores (Ramberg, 1963, 1964; Ghosh, 1968; Johnson and Ellen, 1974; Johnson and Honea, 1975; Ramberg and Johnson, 1976; Dubey and Cobbold, 1977; Fowler and Winsor, 1996).

Mechanical results, based on theoretical or experimental analysis, must be taken into account when constructing an evolutionary model or a theoretical pattern of strain distribution in chevron folds. In this respect, the kinematical models exclusively involving slip or shear parallel to the layer boundaries (Ramsay, 1967, 1974; Ramsay and Huber, 1987) contradict the mechanical arguments above, which suggest a fold development with an important operation of the tangential longitudinal strain folding mechanism (TLS). On the other hand, models like those of de Sitter (1956) and Pollard and Fletcher (2005) involve the operation of TLS in the individual layers so that folding progresses by rotation without straining of the straight limbs, but they do not analyse the strain that occurs in the hinge zone. On this basis, it can be stated that the kinematical mechanisms and the strain patterns inside the layers involved in chevron folding are not yet well understood.

The analysis of the strain distribution in folds can be undertaken using certain geometrical rules (folding mechanisms) that are based on simple experiments (e.g., folding of a competent layer or a card deck; Kuenen and de Sitter, 1938) consistent with observations in natural folds. These mechanisms allow the construction of theoretical folds that can be compared with natural folds in order to provide information about their strain state. However, this approach has some limitations. The folding mechanisms used to model folds and explain the form of the folded layers (flexural flow, flexural slip, tangential longitudinal strain, etc.), are often too simple to fit the strain in specific natural or experimental folds. Probably, a combination of these simple mechanisms operating simultaneous or successively can improve the approximation (Bastida et al., 2003). Even so, some phenomena occurring during folding, such as hinge or neutral line migration (Stewart and Alvarez, 1991; Fowler and Winsor, 1996), can complicate the theoretical modelling of the strain state inside the folded layers.

The present paper investigates two issues: (a) to explore what types of two-dimensional strain distributions can theoretically produce chevron folds; (b) to analyse which of these distributions are likely in competent layers of natural chevrons folds. The first problem is studied by modelling theoretical folds using the program 'FoldModeler' (Bobillo Ares et al., 2004) in a new version, and the second problem is tackled by comparison of the characteristics of the theoretical folds with features observed in natural folds. The present version of 'FoldModeler' allows modelling of folds by tangential longitudinal strain without area change (ETLS) and with area change (PTLS) (Bobillo-Ares et al., 2006), flexural flow (FF), homogeneous layer shortening (LS) and homogeneous flattening (HF).

In addition, the program permits the superposition of a general homogeneous strain (HS), that can be rotational or irrotational and whose principal directions can have any orientation with respect to the geometrical elements of the fold. The superposition of this strain in general produces asymmetric folds.

Although chevron folds are generally developed on multilayers, the present paper is mainly concerned with the strain analysis in individual competent layers, since these control the geometry of folds. Incompetent layers are accommodated in their geometry and strain within the spaces between competent layers and their strain state is difficult to predict at present. Nevertheless, a complete understanding of the deformation involved in the development of chevron folds requires knowledge of the discrete displacements between adjacent layers; an issue that will be discussed further in this paper.

2. Some structural features of natural chevron folds

Chevron folds at different locations (mainly Hartland Quay, Devon, UK; Millook Haven, Cornwall, UK; Barrika, Biscay, Spain; and several areas of Asturias, Spain), together with pictures and descriptions from the geological literature, have been analysed to gain insight into the characteristics of natural chevron folds. The studied chevron folds developed under conditions ranging between diagenetic and greenschist facies (chlorite zone). To analyse the microstructures and strain in the competent layers, samples have been collected from the hinge zones (outer and inner arcs) and the limbs of two folds (one from Millook Haven and another one from Cape Peñes area, Asturias). The samples of Millook Haven are greywackes and those from Cape Peñes are quartzarenites.

Competence contrast is usually high in the multilayers where the studied chevron folds develop. This contrast is indicated by the presence of common veins and fractures and the rare development of cleavage in the competent layers of the sequence. Wedge shaped veins widening towards the outer arc are abundant in the hinge zones of natural chevron folds (Fig. 2). These structures indicate operation of the brittle equivalent of a mechanism of PTLS (Hudleston and Srivastava, 1997; Bobillo-Ares et al., 2006). An estimate of the increase in area

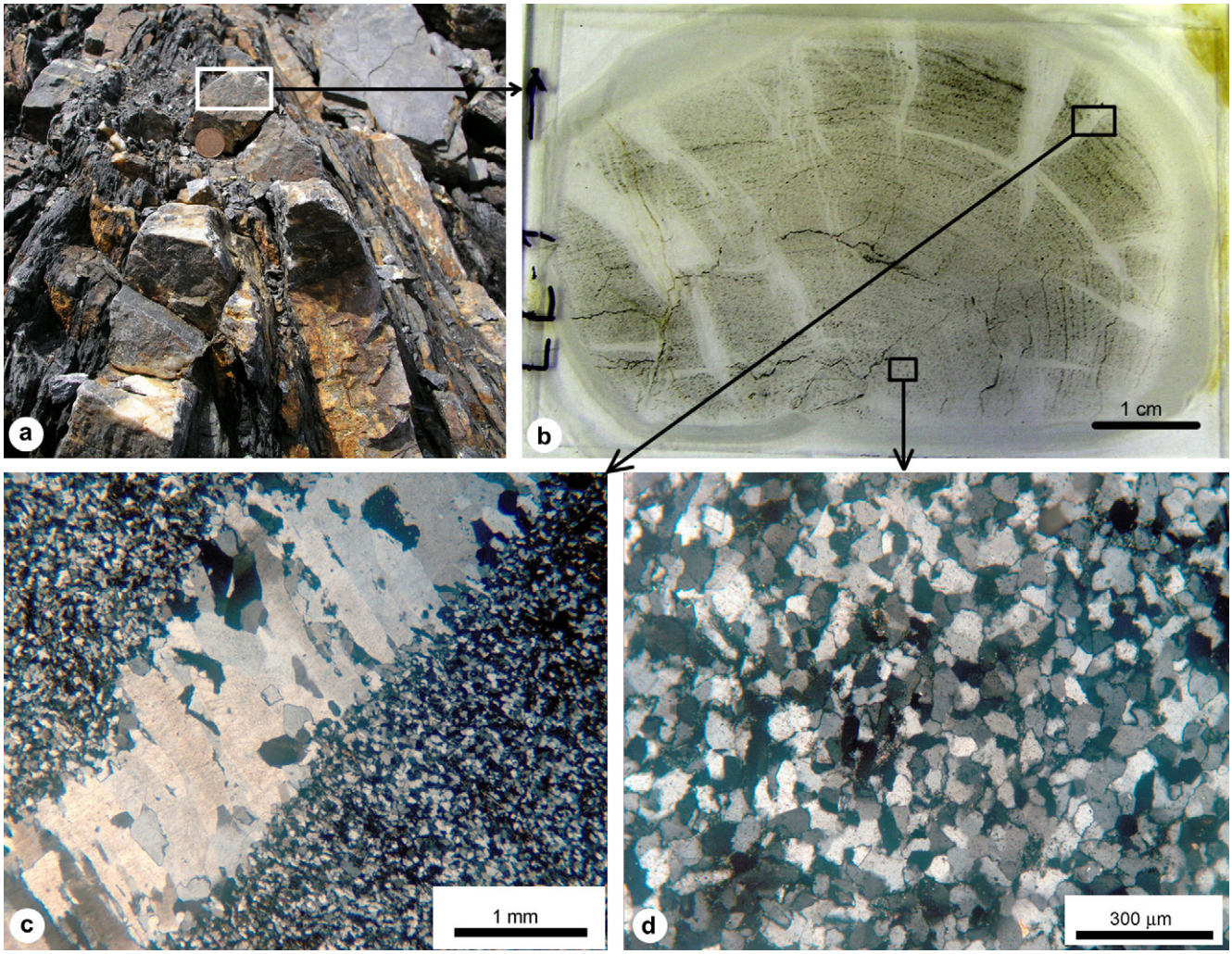

Fig. 2. (a) Chevron fold in Silurian sandstone and shale (Cape Peñes area, Asturias, Spain). (b) Thin section of a sample collected in the hinge zone; it presents abundant wedge shaped veins opening towards the outer arc. (c) Microphotograph of a detail near the outer arc of the folded layer. (c) Microphotograph of a detail near the inner arc of the folded layer.

and length associated with the development of these veins has been made on the sample collected from a chevron hinge zone of the Cape Peñes area (Fig. 2). In this case, the tangential stretch ($\sqrt{\lambda_1}$) varies from 1.53 in the outer boundary to 1.02 in the middle part of the layer, whereas the area change (J = final area/initial area) decreases from 1.46 near the outer boundary to 1.15 in the middle part of the layer. In the case of a chevron fold illustrated by Ramsay and Huber (1987, p. 459), values of $J = 1.56$ are obtained for the outer arc using a similar procedure. These data do not consider ductile deformation of the rocks and give only indicative minimum values, but shed some light on the magnitude of area change in the outer arc during the development of some natural chevron folds. Under the microscope, microstructures of plastic intracrystalline deformation or cataclastic flow are scarce in the outer arc and on the limbs of the folds analysed.

At outcrop, in the studied folds, structures indicating tangential shortening in the inner arc are less apparent that dilatational structures of the outer arc. Nevertheless, cleavage parallel to the axial plane or with a convergent fan pattern is found in some cases affecting mainly the hinge zone inner arc. In the Millook Haven fold, the thin sections from or near the inner arc show an irregularly developed pressure solution cleavage parallel to the axial plane or with a weakly convergent fan pattern (Fig. 3a–c). All these observations again suggest a mechanism of PTLS. Strain measurements by Fry's method (Fry, 1979) show the existence of domains with a very small strain ratio ($R = \sqrt{\lambda_1/\lambda_2} \approx 1$) and domains with a moderate strain ratio ($R < 1.9$) (Fig. 3d). Similar values have been obtained by Yang and Gray (1994) in chevron folds of the Bendigo-Ballarat area (SE Australia). The thin sections from Cape Peñes quartzarenites exhibit no shape preferred orientation of the grains and only scarce microstructures indicative of plastic intracrystalline deformation in chevron fold inner arcs. Other compressional structures, like bed-normal stylolites or reverse faults, can be also found occasionally in the inner arcs of the Cape Peñes chevron folds. In any case, these are minor features that involve a small deformation. The obtained low or moderate R values contrast with the predictions of the mechanical models; this inconsistency could be due to the possible operation of a mechanism, such as grain-boundary sliding, which is undetectable from strain measurements. Evidence of cataclastic flow is not present in the inner arcs of the studied folds.

Crystals of fibrous quartz or calcite are common on bedding surfaces in the limbs of chevron folds; in most cases, the fibre direction forms a high angle with the fold axis and the directional sense of movement agrees with inter-layer slip linked to the folding. It is also frequent to find accommodation structures, such as bulbous hinges, limb faults, boudinage, hinge collapses, saddle reefs or faults along the axial surface.

Although we can see only the final form in natural chevron folds, it is possible to observe some features in the field that suggest how these folds could have developed from rounded folds in some cases. For example, in the beach section of Hartland Quay (Devon) there is a train of upright close chevron folds (Fig. 4) with a gentle rounded antiform in the northern end. This geometry suggests that during the first stages of folding, the folds had a rounded shape and they acquired the chevron shape later. On the other hand, sometimes it is possible to observe rounded folds that become angular folds towards the core. In the example of Fig. 5a, two chevron antiforms are separated by a rounded wide synform; this geometry is comparable to that described theoretically by Johnson and Honea (1975) (Fig. 5b) and to the results of the experiments cited in the previous section, in which the chevron folds develop from the core of the concentric folds.

3. Modelling methods

Chevron folds formed by different kinematical folding mechanisms can be modelled using the appropriate transformation relations of points developed by Bobillo-Ares et al. (2000, 2004, 2006) and Bastida et al. (2003). We have applied the transformations using a new version of the computer program 'FoldModeler' (Bobillo-Ares et al., 2004). This program starts from the initial configuration of a layer profile formed by a grid of parallelograms. The nodes of the grid are then displaced according to the transformation relations of the mechanisms involved in folding, and the layer shape is obtained. In addition, the strain pattern is determined by comparative analysis of the folded and original configurations.

In the modelling carried out with 'FoldModeler', it is necessary to initially define the ''guideline'', a longitudinal reference line located inside the layer that enables the monitoring of folding. In the models, this line has been initially located in the middle of the layer, except in those cases indicated. The shape of the guideline must be defined by a mathematical function, and the functions used in this paper are the conic sections (Aller et al., 2004). The part of a conic section used to represent the fold guideline can be defined by its eccentricity e, which is the distance from a general point of the conical curve (P) to a fixed point (focus, O) divided by the distance from P to a fixed straight line (directrix) ($0 \leq e < 1$, ellipse; $e = 1$, parabola; $e > 1$, hyperbola), and the aspect ratios h of the limbs, defined as the ratio between the height y_f and the width x_f of the limb considered (Fig. 6). In the new version of 'FoldModeler', the two limbs of the fold must be modelled together, since the superposition of a general HS commonly produces asymmetric folds involving migration of the hinge point along the guideline; as a result, a point can pass from one limb to the other during the development of the fold. Then, it is convenient to describe the guideline using a single conic section for the two limbs, since this facilitates the analytical description of the conic section after the superposition of the HS. The problem is reduced in this case to finding the new hinge point (vertex of the conic), fix the origin of a new coordinate system at it and find the new equation of the conic section.

Modelling of folds is made by successive or simultaneous superposition of folding steps. Each folding step is defined according to the mechanism applied, the increment that it

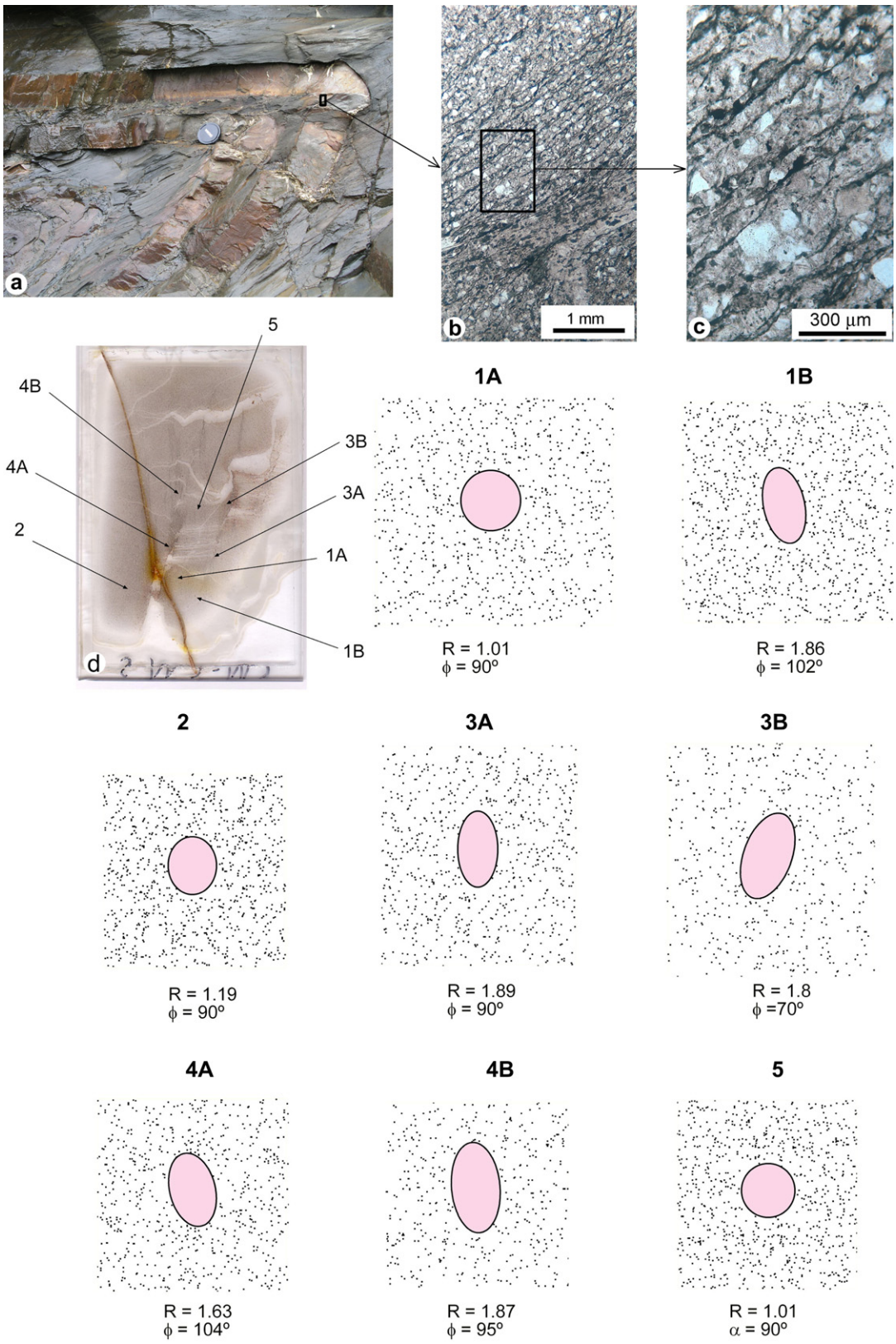

Fig. 3. (a) Chevron fold in Carboniferous greywacke and shale (Millook Haven, Cornwall, SE England). (b) and (c) Microphotographs taken from a sample collected near the inner arc of the folded layer; they show the presence of a pressure solution cleavage. (d) Thin section from a sample located near the inner arc with the results of the strain measure by Fry's method at several points.

Fig. 4. Folds in Carboniferous greywacke and shale (Hartland Quay, Devon, SE England). The folds with minor amplitude, located at the northern end of the section (north towards the left), are rounded; the rest of the folds are chevron.

produces in terms of the aspect ratio h, and the change that it produces in the shape of the guideline, characterised by the eccentricity of the conic section that defines the guideline. The simultaneous superposition of several mechanisms can be modelled by applying a large number of successive steps of the mechanisms considered with very small increments in the aspect ratio and shape of the guideline.

For the analysis of the strain state in the folded layer, the program 'FoldModeler' allows the construction of curves that show the variation of R (amount of strain defined as $R = \sqrt{\lambda_1/\lambda_2}$, where λ_1 and λ_2 are the principal quadratic elongations of the strain), J (area strain, defined as $J =$ final area/initial area) and ϕ (inclination of the long axis of the strain ellipse), along the inner and outer arc of the folded layer, as a function of the dip α. Fig. 6 shows the sign convention for the angles ϕ and α.

4. Kinematical models for the development of chevron folds

4.1. Folding by flexural flow

Chevron folds can in principle be modelled by using different kinematical mechanisms. Ramsay (1967, 1974) and Ramsay and Huber (1987) used flexural flow (FF) to explain the geometry of these folds in competent layers. A chevron fold modelled with 'FoldModeler' using this mechanism can be seen in Fig. 7. It is a parallel fold in which the ratio R increases from the hinge zone ($R = 1$, no strain) towards the limbs, where the strain pattern involves high shear strain parallel to the layer boundaries. The model is perfectly possible from a geometrical point of view, but it seems mechanically unrealistic. It was criticized by Bayly (1976) who stated that for chevron folds developed in non-foliated competent rocks, which are approximately isotropic materials, it is difficult to produce internal shear displacements parallel to the layer boundaries. A similar conclusion about the role of flexural flow in folds formed in competent layers was reached by Hudleston et al. (1996). Moreover, the mechanical models of "chevron folds" involving a non-linear rheological behaviour predict a yielding in the hinge zone, where R must therefore reach the highest values. Finally, the strain pattern of the flexural flow is not compatible with the associated minor structures that usually appear in the hinge zone of chevron folds.

4.2. Folding by tangential longitudinal strain

A theoretical chevron fold formed by equiareal tangential longitudinal strain (ETLS) (Ramsay, 1967; Ramsay and Huber, 1987; Bobillo-Ares et al., 2000), is shown in Fig. 8. To produce this fold it is necessary to consider that the neutral line is located at the inner arc boundary of the folded layer. With any other position of the neutral line, a bulge appears in the inner arc of the hinge zone, a feature that is not common in chevron folds. In this model, large extensional strains and

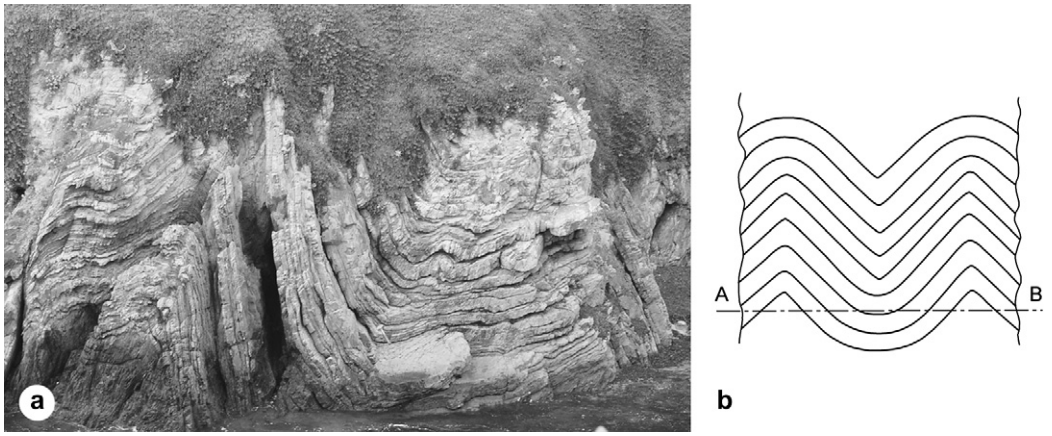

Fig. 5. (a) Folds in Cambrian-Ordovician sandstone (Tapia de Casariego, Asturias; Spain). The antiforms in the ends of the section are close to chevron folds, whereas the synform between them is a rounded fold. (b) Sketch showing the theoretical formation of chevron folds in the core of concentric folds. Section A-B approximates the geometry of the folds in the picture (after Johnson end Honea, 1975; slightly modified).

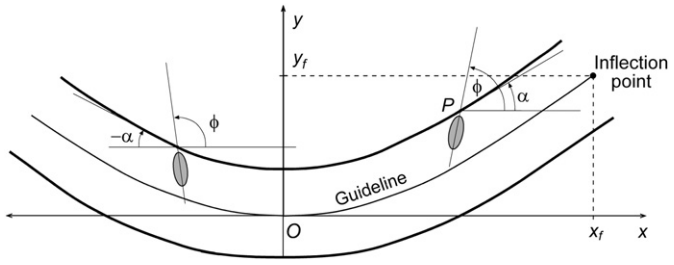

Fig. 6. Sign convention for angles ϕ and α.

a drastic thickness decrease appear in the hinge zone. These features are not found in the natural chevron folds analysed.

Parallel tangential longitudinal strain (PTLS), which produces no stretching of lines in the direction orthogonal to the layer and therefore results in area change and in perfect class 1B folds (Hudleston and Srivastava, 1997; Bobillo-Ares et al., 2006), gives perfect chevron folds in many respects. In this model, area decrease in the inner arc of the hinge zone prevents the development of the bulge; this combines with area increase in the outer arc (Fig. 9). Strain is concentrated in the hinge zone as the mechanical studies suggest, but the implied area changes in this zone are very high (80% close to the layer boundaries of the model in Fig. 9, and in general >70% for interlimb angles <90°) and seem improbable in natural chevron folds.

A sequence with ETLS followed by PTLS can give rise to chevron folds, but if the application order is reversed we have a situation similar to that with a single event of ETLS, since the problems posed by the latter mechanism depend on the curvature increment of the guideline, and this increment is high in the late stages of the fold development. Nevertheless, ETLS-PTLS sequences still produce high strain values ($R > 5$ in general) and unrealistic area decreases (minimum 70%) in the inner arc. The advantages of models with dominant PTLS are the strain concentration in the hinge zone, compatible with mechanical predictions, and the formation of a convergent fan of the major axes of the strain ellipse in the inner arc, which is a feature found in natural folds.

4.3. Folding by superposition of tangential longitudinal strain and flexural flow

It seems difficult to obtain a geologically probable chevron fold by the operation of only one or two folding mechanisms. The possibilities to model chevron folds by combination of more than two mechanisms are infinite. Fortunately, the characteristics of natural chevron folds and the mechanical models

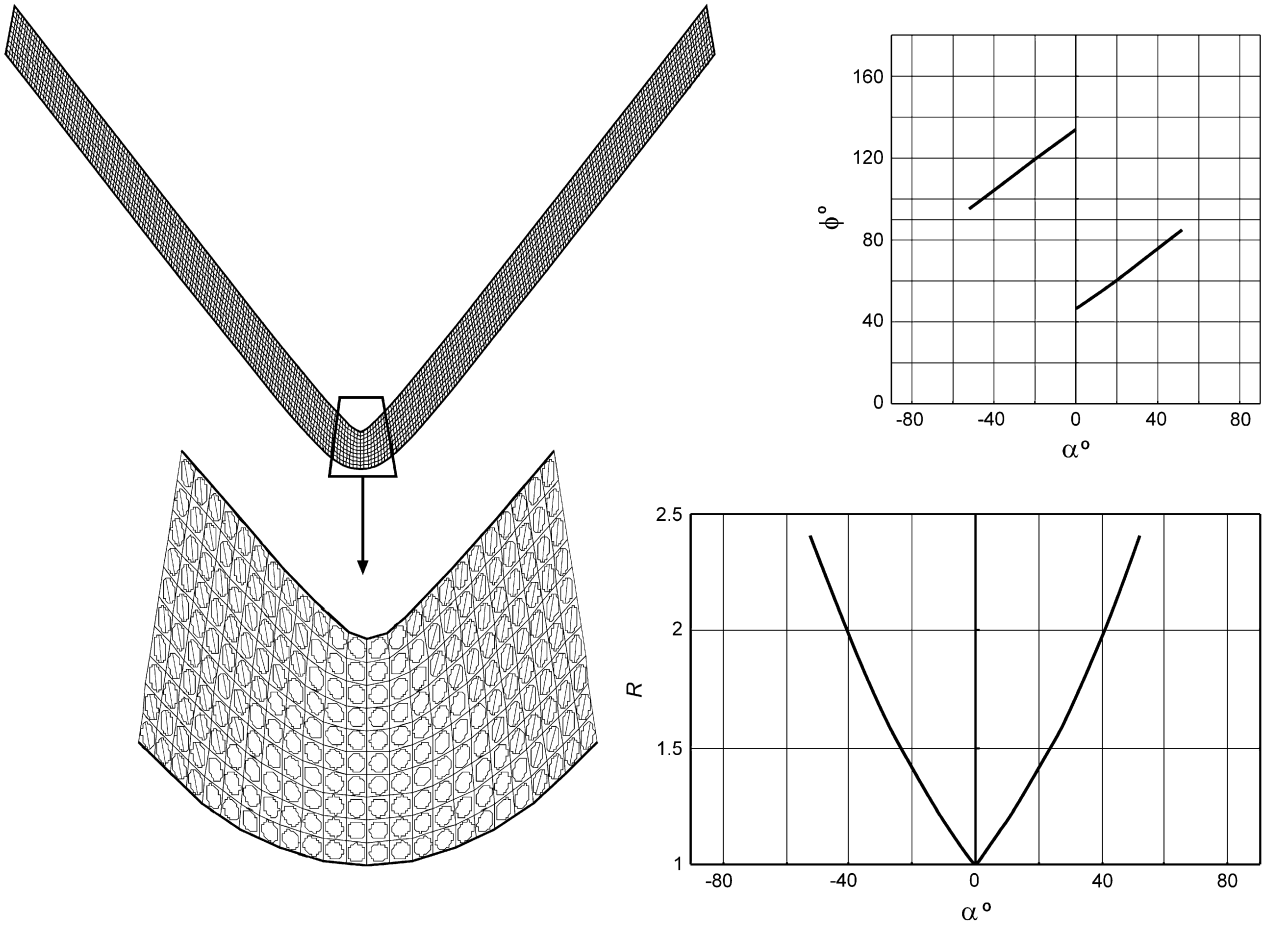

Fig. 7. Chevron fold modelled by FF. In the detailed drawing of the hinge zone, the strain ellipses and their long axes are shown when $R \geq 2$, indicating areas where cleavage would be probable. Aspect ratio $h = 1.2$, eccentricity of the guideline $e = 1.266$.

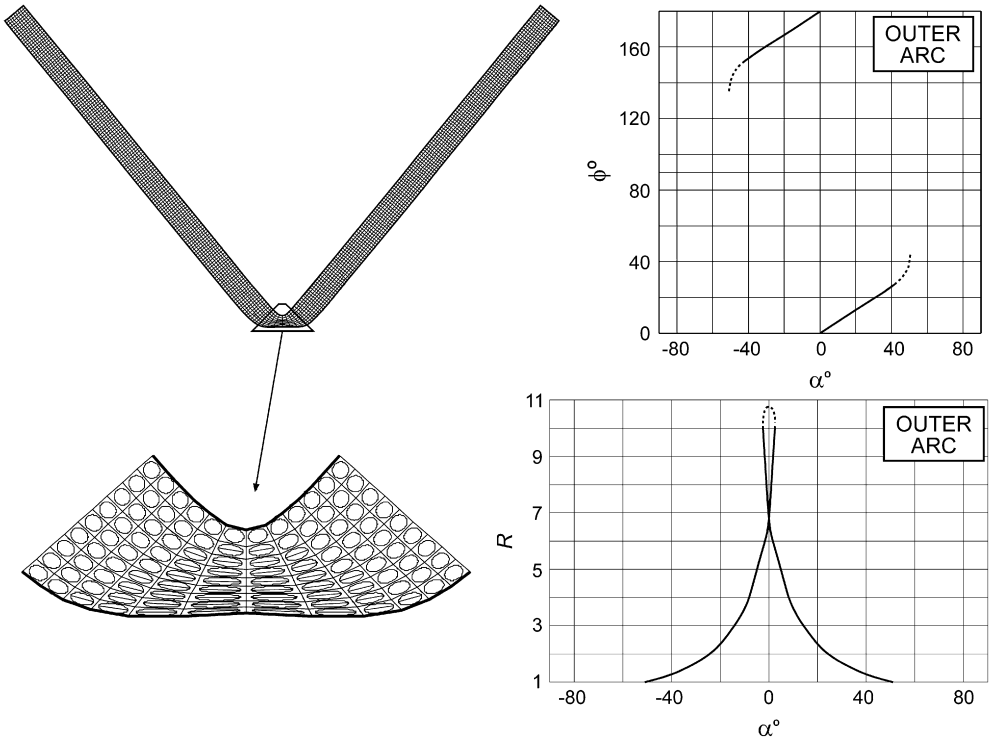

Fig. 8. Chevron fold modelled by ETLS. The guideline coincides with the inner arc of the layer. In the detailed drawing of the hinge zone, the strain ellipses and their long axes are shown when $R \geq 2$, indicating areas where cleavage would be probable. Aspect ratio $h = 1.2$, eccentricity of the guideline $e = 1.29$.

that explain their formation impose severe constraints on the amount and the order of the operating mechanisms. A first constraint imposed by the modelling is that the chevron folds must reach their angular shape from rounded folds (Fig. 10); it agrees with mechanical models for the development of chevron folds (Johnson and Honea, 1975). A sequence beginning as chevron folds would produce geologically unfeasible strain and/or area changes. After a detailed analysis of chevron fold models, we conclude that sequences involving a first stage of ETLS, and a second stage with different combinations of PTLS and FF can be considered representative of the different combinations of buckling mechanisms that can yield geologically feasible chevron folds. This sequence avoids the problems posed by ETLS in the late stages of folding. Furthermore, the operation of FF in the late stages of folding prevents the huge strain and area change that PTLS alone would produce in the hinge area.

Some examples have been modelled to analyse the contributions made by the different mechanisms in the sequences ETLS-PTLS-FF, ETLS-FF-PTLS, and ETLS-simultaneous PTLS and FF. A set of examples has been made with a constant e value of 1.264 and a finite aspect ratio of 1.2. The aspect ratio of the ETLS step has been set to 0.7 (58% of the final amplitude). Lower amplitudes of this step have to be compensated by a higher percentage of PTLS that produces area changes that are unreasonably high, whereas higher amplitudes of the ETLS step produce strains too high in the inner arc. The total aspect ratio of the second event with PTLS and FF has been set to 0.5 (42% of the total amplitude). Fig. 11 shows the results obtained for several characteristic properties as a function of the FF percent; these properties are: dip angle of the major axis of the strain ellipse for the limb dip of 20° in the inner arc (Fig. 11a), R value for the limb dip of 0° in the inner arc (Fig. 11b), and maximum and minimum dilation in the outer and the inner arc respectively (Fig. 11c). Taking into account features commonly observed in natural chevron folds, such as convergent cleavage fans in the hinge inner arc and moderate R and area change values, some of the sequences represented in Fig. 11 can be discarded as unrealistic, like those with $\phi < 80°$ (right limb) and $\phi > 100°$ (left limb), $R > 4$, and $|\Delta|(\%) > 70$. Combining the three diagrams of Fig. 11 we infer that sequences that give rise to folds compatible with geological observations are: ETLS-PTLS-FF with FF between 3 and 18%, ETLS-simultaneous PTLS and FF with FF between 23 and 36%, and ETLS-FF-PTLS with FF about 39%.

Another set of examples has been made with a constant e value of 1.165 and a finite aspect ratio of 1.5. The aspect ratio of the ETLS step has been set to 0.9 (60% of the final amplitude). In this case, the sequences compatible with geological data are: ETLS-PTLS-FF with FF between 4% and 26%, ETLS-simultaneous PTLS and FF with FF between 26 and 37%, and ETLS-FF-PTLS with FF about 38%. Only small differences exist between these values and those obtained for the set of examples with finite aspect ratio of 1.2. In all cases, the upper limit of the FF intervals is controlled by the divergence in the pattern of the long axes of the strain ellipses produced by this mechanism in the inner arc. In general, the sequence ETLS-FF-PTLS seems less appropriate, since it produces cleavage fans that are more divergent in the inner arc

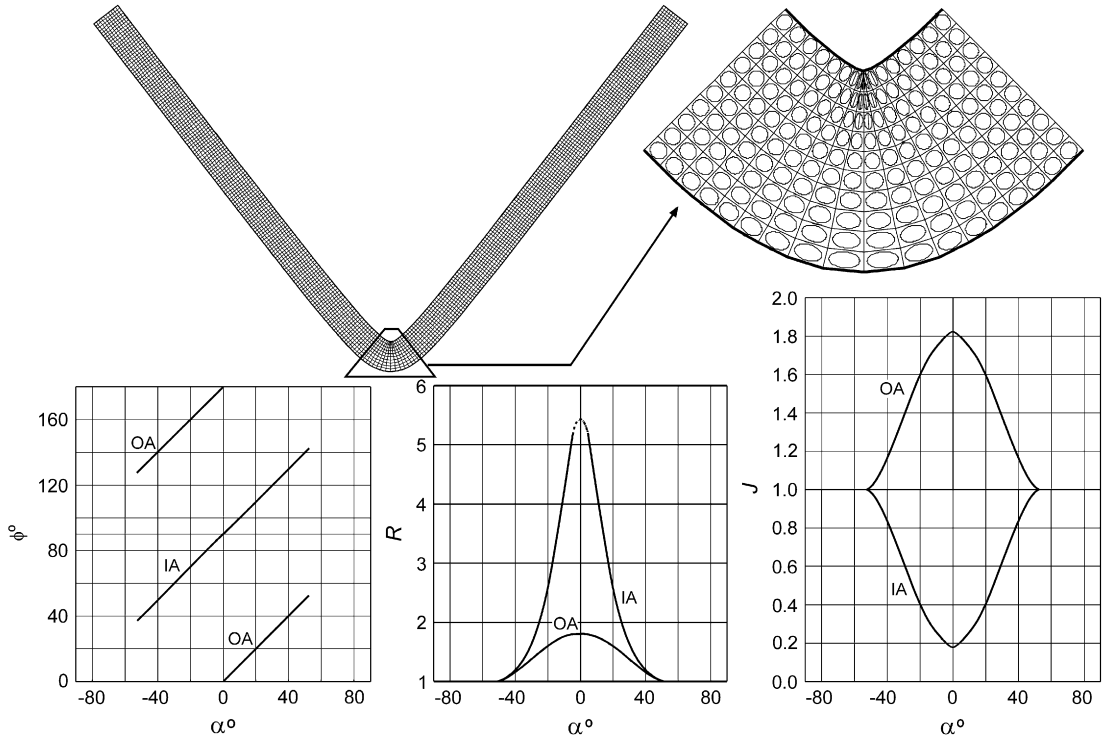

Fig. 9. Chevron fold modelled by PTLS. In the detailed drawing of the hinge zone, the strain ellipses and their long axes are shown when $R \geq 2$, indicating areas where cleavage would be probable. Aspect ratio $h = 1.2$, eccentricity of the guideline $e = 1.26$. IA, inner arc; OA, outer arc.

than those obtained with the other sequences. A representative example of a fold formed by the ETLS-PTLS-FF sequence with 6% of FF and aspect ratio 1.2 is shown in Fig. 12. Folds modelled by a sequence ETLS-simultaneous PTLS and FF deliver results quite similar to those obtained by the sequence ETLS-PTLS-FF.

Fig. 10 shows the progressive evolution of a fold formed by the ETLS-PTLS-FF sequence with 6% component of FF. The maximum dip (α) vs. normalised amplitude (h) curve shows that the final h increment due to FF that produces the chevron shape is associated with a very small variation of the maximum limb dip (α), which explains the very small FF strain produced in the straight part of the limb.

In the models above, the chevron shape is developed in the final folding step. Nevertheless, in natural folds it cannot be ruled out that the chevron morphology appears early in the folding process with the final amplification only preserving this shape. Modelling sequences of this type require at least

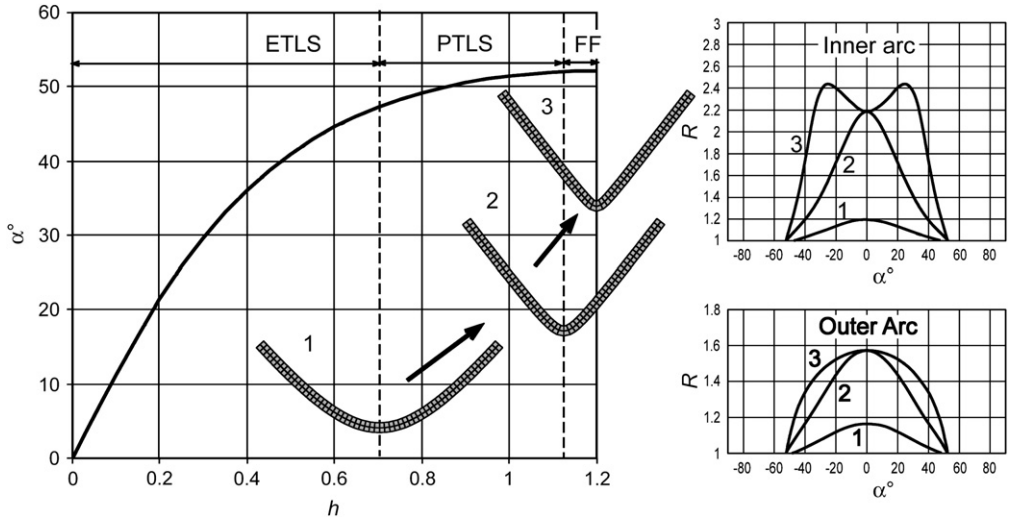

Fig. 10. Evolution of the shape of a chevron fold modelled by a sequence ETLS-PTLS-FF. Curves of α in the limb against h, and R against α in the inner and the outer arc for the three folding steps are also shown. Eccentricity of the guideline $e = 1.264$.

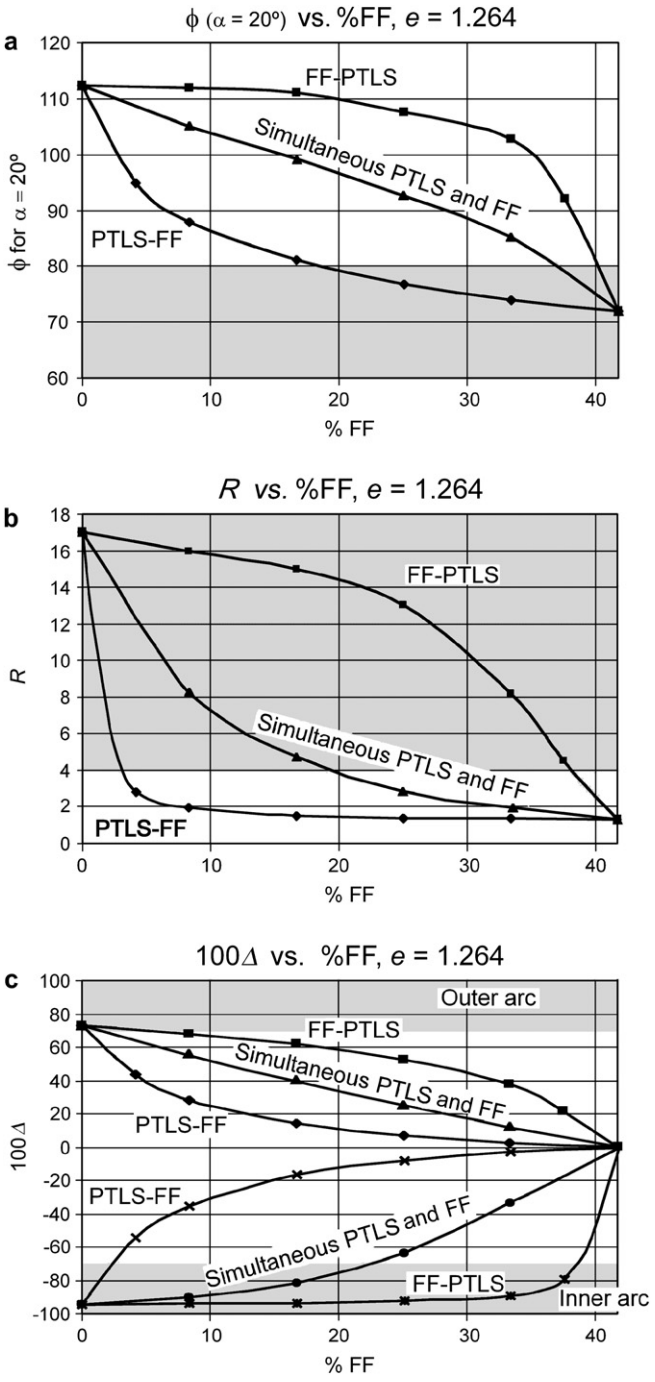

Fig. 11. Curves of ϕ (for $\alpha = 20°$) (a), R (for $\alpha = 0$) (b), and Δ (for $\alpha = 0$) (c) against the percent of the aspect ratio produced by FF for folding sequences ETLS-FF-PTLS, ETLS-simultaneous PTLS and FF and ETLS-PTLS-FF. The curves in (a) and (b) correspond to the inner arc. e is the eccentricity of the conic section that defines the guideline.

two steps of chevron folding that must have a variable e value. An example of this type of folds, developed with a sequence ETLS-PTLS-FF, in which the chevron fold is formed in the second folding step, is shown in Fig. 13. This sequence gives results comparable to those obtained with PTLS (Fig. 9) or with the sequence ETLS-PTLS, and involves very high J and R values in the hinge zone inner arc. A decrease of the J and R values in the hinge zone can be obtained with the sequence ETLS-PTLS-FF-FF, in which the chevron form is developed during the first FF step. Nevertheless, this sequence poses the same problems as the sequences with dominant FF, such as the divergent cleavage fan produced in the hinge zone inner arc. It can be concluded that once the chevron shape has developed, it is probable that only homogeneous deformation can be a significant mechanism to continue folding in natural folds, since further growth of the fold by TLS gives rise to excessive strain and area change values in the hinge zone, whereas FF produces folds with a divergent fan pattern of the long axes of the deformation ellipses in the hinge zone inner arc.

4.4. Application of homogeneous strain

Incorporation of a step of homogeneous layer parallel shortening (LS) prior to the folding sequence that gives rise to chevron folds has some implications on the final folds produced. An example with the sequence LS-ETLS-PTLS-FF is shown in Fig. 14. The main effect observed is the tendency towards a convergent distribution of the major axes of the strain ellipse. This convergent distribution extends from the inner to the outer arc with increasing values of R of the LS, as the final strain ellipse evolves in the outer arc from one of tangential stretching to one of tangential shortening. Some of the characteristics found in this model, like the convergent cleavage in the hinge zone inner arc, resemble features observed in natural chevron folds.

Existence of an episode of homogeneous strain (HS) at the end of folding seems likely to have contributed to the formation of many natural chevron folds. When the chevron fold reaches an interlimb angle of about 60°, the continuation of buckling requires excessive amounts of slip between beds (de Sitter, 1958; Ramsay, 1967, 1974), and HS is a probable mechanism to allow continued deformation whilst preserving the chevron morphology. On the other hand, as amplitude increases, the models of chevron folds described previously give rise in general to large area changes that hinder the progression of folding and can also favour a mechanism of HS. HS with maximum shortening perpendicular to the axial plane (homogeneous fold flattening, HF) is probably a common mechanism in natural chevron folds. This mechanism produces an increase in the normalised amplitude h of the fold and a decrease of the interlimb angle (Fig. 15). It also produces a decrease in the ratio between the limb and the hinge thickness (class 1C folds; Ramsay, 1967) and a generalised increase in the R values throughout the fold, which only excludes the hinge zone outer arc in some cases. Moreover, HF changes the distribution of the major axes of the strain ellipses towards an axial planar pattern, mainly in the inner arc. All these characteristics are accentuated as the strain ratio, R, of the HF increases.

Hudleston (1973) has argued that flattening can occur simultaneously with buckling when the ductility contrast between layers is low, but this is hardly applicable to most chevron folds, which are developed in multilayers with high ductility contrast.

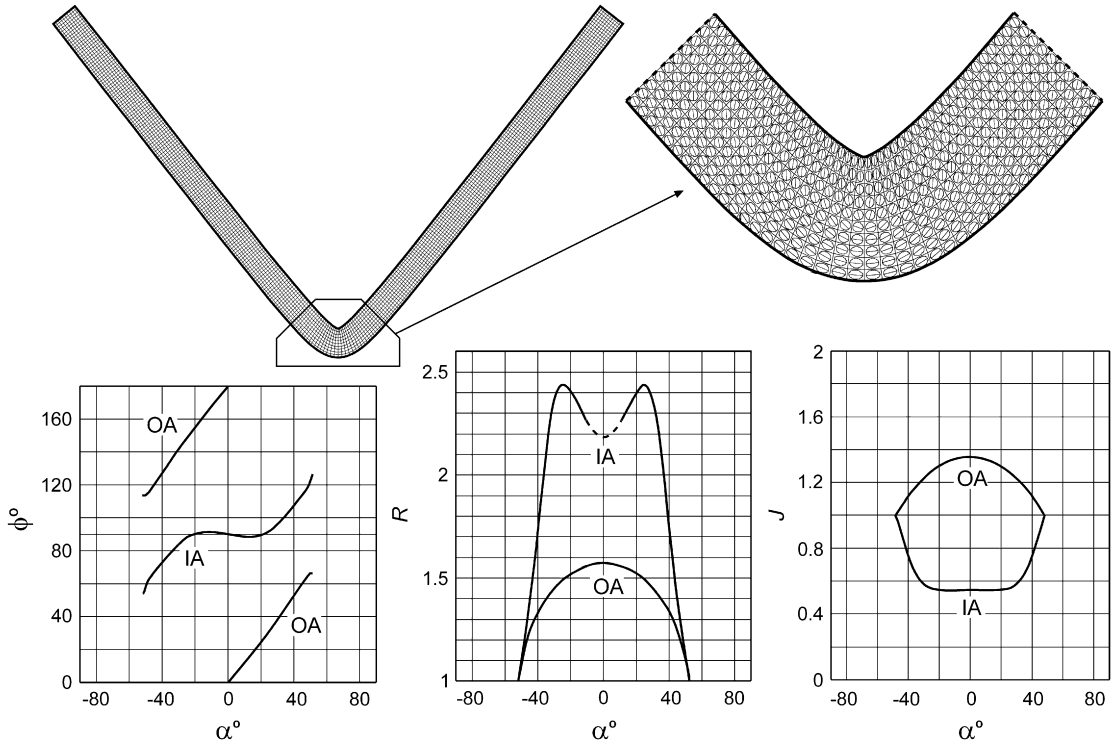

Fig. 12. Chevron fold modelled by a sequence ETLS-PTLS-FF. The strain ellipses are shown in the detail drawing of the hinge zone. Aspect ratio $h = 1.2$, eccentricity of the guideline $e = 1.264$. IA, inner arc; OA, outer arc.

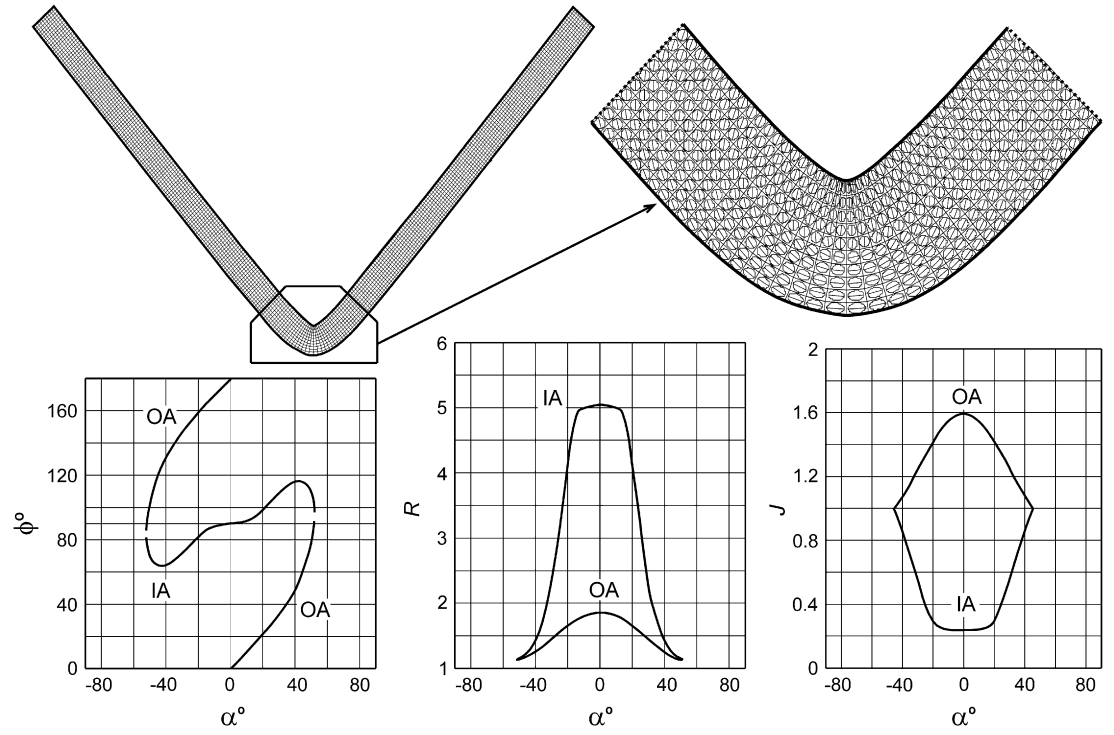

Fig. 13. Chevron fold modelled by a sequence ETLS-PTLS-FF in which the chevron shape is introduced in the PTLS folding step. The strain ellipses and their long axes are shown in the detailed drawing of the hinge zone. Aspect ratio $h = 1.2$. Eccentricity of the guideline: ETLS step $e_1 = 1.264$, PTLS step $e_2 = 1.304$, FF step $e_3 = 1.264$. IA, inner arc; OA, outer arc.

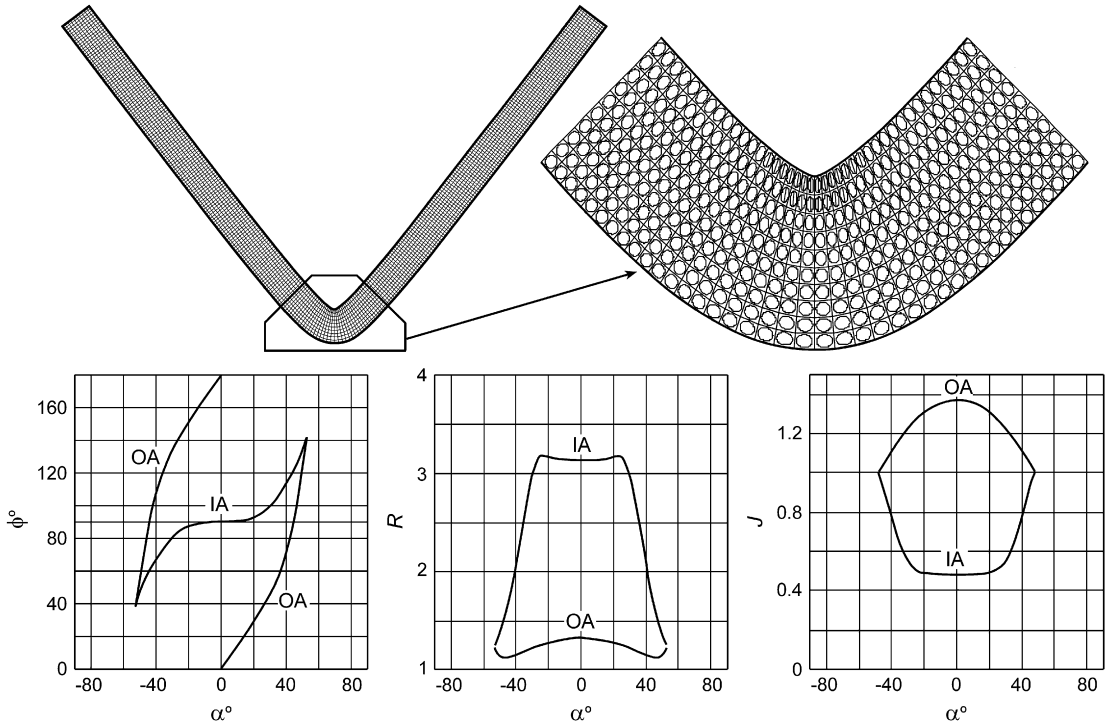

Fig. 14. Chevron fold modelled by a sequence LS-ETLS-PTLS-FF. LS with $\sqrt{\lambda_2} = 0.9$ and without area change. Aspect ratio $h = 1.2$, eccentricity of the guideline $e = 1.255$. In the detailed drawing of the hinge zone, the strain ellipses and their long axes are shown when $R \geq 2$, indicating areas where cleavage would be probable. IA, inner arc; OA, outer arc.

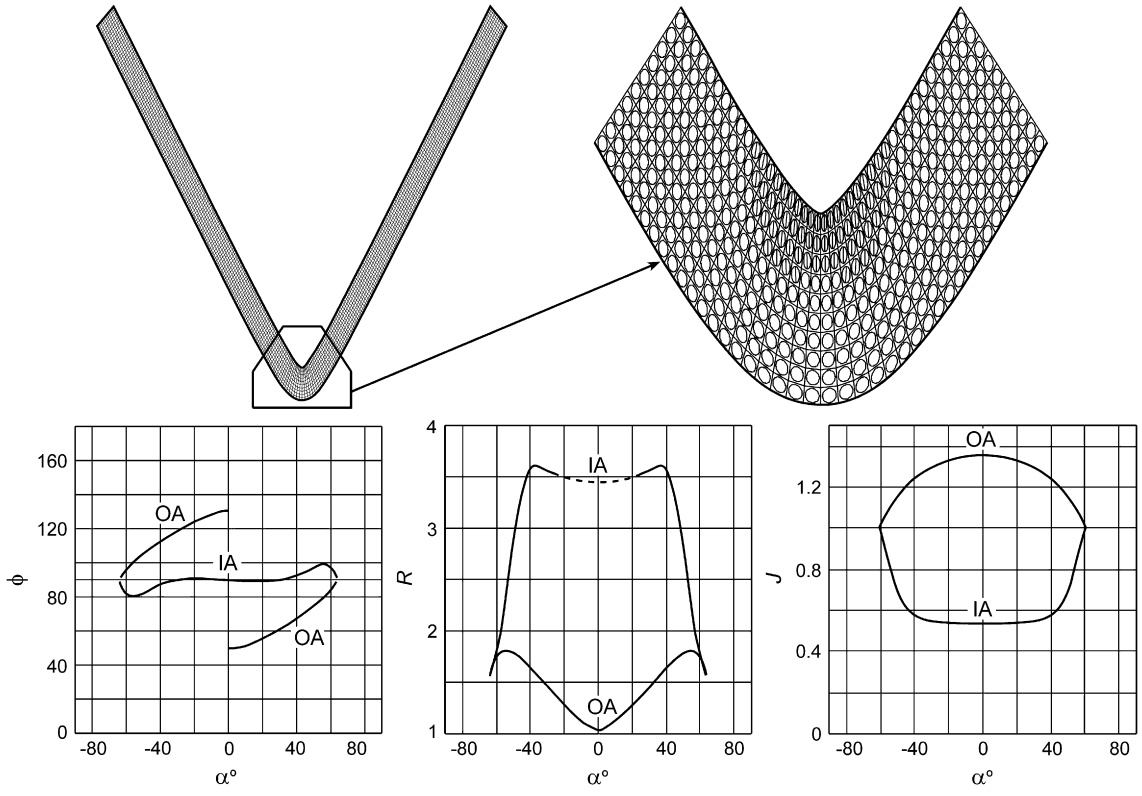

Fig. 15. Chevron fold modelled by a sequence ETLS-PTLS-FF-HF. HF with $\sqrt{\lambda_2} = 0.8$ and without area change. In the detailed drawing of the hinge zone, the strain ellipses and their long axes are shown when $R \geq 2$, indicating areas where cleavage would be probable. Aspect ratio $h = 1.875$, eccentricity of the final guideline $e = 1.116$. IA, inner arc; OA, outer arc.

In addition, the flattening produces a layer thickening in the hinge zone, which involves an increase of the buckling resistance of the layer (Johnson, 1970, p. 297). Hence, it seems improbable that flattening simultaneous with buckling plays a relevant role in the development of chevron folds.

Superposition of non-coaxial strain on chevron folds is probably very common in natural environments (Ez, 2000; Carreras et al., 2005). A result of this superposition is the development of asymmetric chevron folds. Excellent examples of this type of fold can be found in Millook Haven (Cornwall, UK). They are close recumbent asymmetric chevron folds with the hinge slightly thickened with respect to the limbs and the normal limbs thicker than the reverse limbs (Fig. 1). In Fig. 16, a fold with geometry comparable to the chevron folds of Millook Haven has been modelled by ETLS + PTLS + FF + rotation + simple shear. The four first steps could involve a buckling plus rotation event induced in a general regime of simple shear. We can observe the asymmetrical character of the folded layer; this character is also observed in the curves of ϕ, R and J vs. α. Nevertheless, the modelled fold is an overturned fold, whereas the chevron folds of Millook Haven are recumbent. Therefore, it is necessary to add a tilt to the modelled fold to improve the match. The geometry and the strain pattern of the folded layer of this figure are only a possible approximation to those of the Millook Haven folds. The geometrical similarity between theoretical and natural folds is not sufficient to explain the natural folding mechanisms, and strain measurements are required to improve the approximation. Unfortunately, strain values shown in Fig. 3 are lower than those involved in the theoretical modelling of chevron folds. We will discuss this inconsistency below.

5. Deformation in the multilayer

A complete understanding of strain patterns in chevron folds requires the consideration of the whole multilayer stack where these structures develop. If the multilayer is only formed by competent layers of uniform thickness, it is sufficient to consider two adjacent layers. 'FoldModeler' does not allow the modelling of folding in multilayers, but we can model a single layer and then juxtapose it to another one modelled with the same geometrical parameters in order to analyse some geometrical properties of the set. In Fig. 17, the slip produced between two adjacent competent layers is shown for a chevron fold developed by FF and for another one developed by PTLS. It can be observed that slip between layers appears in folding by FF despite the limb length along the bottom and along the top being the same; this slip is due to the detachment with an associated dilation space that occurs in the hinge zone. Nevertheless, the slip is lower in the chevron

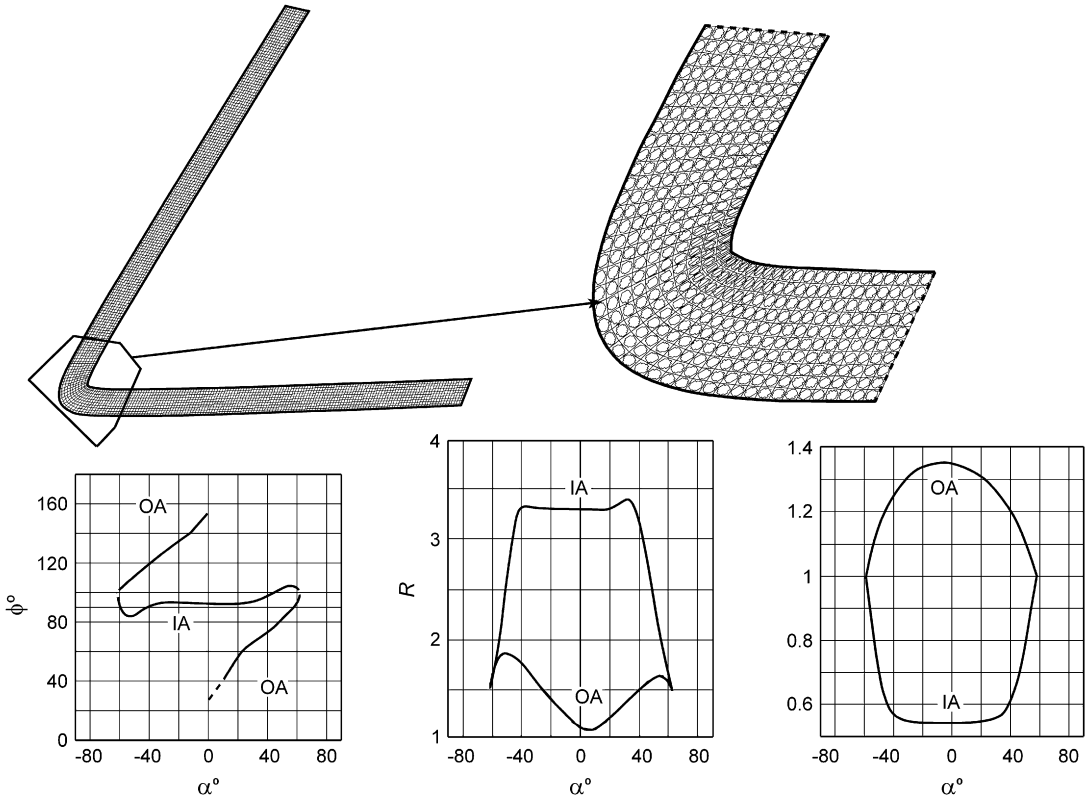

Fig. 16. Asymmetric chevron fold modelled by a sequence ETLS-PTLS-FF-rotation (50°)-HS (simple shear with $\gamma = 0.4$ and a shear direction of 50°). This fold can be considered as a representative model of the chevron folds at Millook Haven. In the detailed drawing of the hinge zone, the strain ellipses and their long axes are shown when $R \geq 2$, indicating areas where cleavage would be probable. Aspect ratio: upper limb $h_1 = 1.75$, lower limb $h_2 = 1.74$; eccentricity of the final guideline $e = 1.133$. IA, inner arc; OA, outer arc.

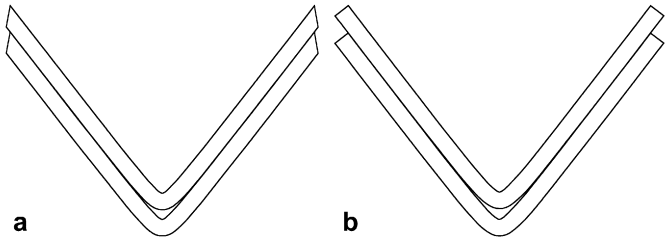

Fig. 17. Slip between two competent layers folded individually by FF (a) and folded by PTLS (b). Aspect ratio $h = 1.2$.

fold produced by FF than in the one produced by PTLS. This result agrees with that obtained from the ideal model of chevron fold proposed by Ramsay (1967, pp. 440–441), in which the outer arc of the hinge is a circular arc. From this model, where the strain in each layer is due to FF, the slip produced is given by (Ramsay, 1967, eq. 7-39):

$$s_{FF} = t(\tan\alpha - \alpha) \quad (1)$$

where t is the thickness of the layers and α the limb dip. Assuming PTLS in the same model, the slip coincides with the total slip of Ramsay (1967, p. 440):

$$s_{PTLS} = t\tan\alpha \quad (2)$$

The slip given by this equation is higher than that corresponding to flexural slip folding ($S_{FS} = t\alpha$; Ramsay, 1967, p. 393), which is again due to the presence of a detachment with dilation space in the hinge zone.

Eqs. (1) and (2) give a good approximation for more general cases, as those shown in Fig. 17, where the shape of the guideline is hyperbolic. Combinations of ETLS, PTLS and FF give rise to slip amounts between the two cases shown in Fig. 17. The insertion of an incompetent layer between the competent layers slightly modifies the model; the changes can be seen in the study made by Ramsay (1974).

The accommodation structures associated with the existence of an anomalously thick or thin layer and those associated with dilation spaces in the hinge zone depend on the limb dip and the layer thickness/limb length ratio of the different layers in the multilayer (Ramsay, 1974), but not on the mechanisms that operate to develop the chevron fold.

6. Discussion and conclusions

The micro- and mesostructural analysis of natural chevron folds, together with the mathematical modelling, suggest that the kinematical development of these folds requires the sequential or simultaneous operation of several mechanisms. Single mechanisms offer advantages and drawbacks for the development of these folds, but only the combination of them can give rise to the characteristics observed in natural folds.

The very strong curvature in the hinge zone of chevron folds hampers the development of these folds by the exclusive operation of equiareal tangential longitudinal strain (ETLS), since this mechanism produces very high strain in the hinge zone's inner arc that leads to the development of bulges or reverse faults in this zone. These features are found in some cases, but they are not common in natural chevron folds. Moreover, they produce a deviation from the perfect chevron shape. Migration of the neutral line towards the inner arc decreases the strain in this zone, but increases it dramatically in the outer arc, producing a sharp thinning in this zone that is never observed in natural folds.

Operation of parallel tangential longitudinal strain (PTLS) avoids the development of bulges or thinning in the hinge zone and gives rise to a perfect chevron shape, but produces high strain and huge area change (>70% for interlimb angles <90°) in the hinge zone. The positive aspect of this mechanism is that it generates convergent cleavage fans in the inner arc similar to those found in natural chevron folds.

Flexural flow (FF) gives rise to chevron folds with perfect parallel style without area change and without strain in the hinge zone, but some of the characteristics of these folds are not in agreement with the features of natural chevron folds. The lack of strain and the divergent distribution of the strain ellipse major axes in the hinge zone of these theoretical folds contradict the common presence of veins and cleavage in this zone and the convergent distribution of cleavage in natural folds. Moreover, flexural flow involves high shear strain in the limbs parallel to the layer boundaries, which are probably inhibited by the lack of an appropriate mechanical anisotropy in the competent layers (Bayly, 1976; Hudleston et al., 1996).

Theoretical modelling of chevron folds can be made by infinite combinations of kinematical mechanisms. Nevertheless, the features usually observed in natural folds pose some constraints in this respect. A first constraint imposed by mechanical and kinematical models is that chevron folds must evolve from rounded folds. Evolution from an initial chevron fold produces huge strain and area change in the hinge zone inner arc that can only be avoided with the exclusive operation of FF along all the folding process.

If the participation of several mechanisms is considered, the first possible mechanism according to buckling theory is homogeneous layer parallel shortening (LS) (Ramberg, 1964; Hudleston and Stephansson, 1973). Its operation favours the development of convergent cleavage, but is limited by the high competence contrast that the multilayers developing chevron folds usually present.

Simultaneously with or after LS the more probable mechanism is ETLS. In the early stages of folding this mechanism is viable, since the small curvature increments does not involve large strain, and this can be accommodated without area change. On the other hand, PTLS or FF at this stage would give rise respectively to area changes and strain in the limbs of the final fold too high to be geologically realistic.

After folding by ETLS, probable mechanisms are PTLS and FF, which can operate in this order or simultaneously. Modelling shows that sequences FF-PTLS are improbable, since they produce huge strain and area change in the hinge zone. In general, FF is necessary at the late stage of

buckling, although the increment of folding due to this mechanism can be very small. In this late stage, the dip increment in the limbs is very small, and FF strain concentrates near the hinge zone.

High values of slip between layers and area change emerging in the late stage of chevron folding can lead to the end of buckling, probably for an interlimb angle value of about 60°, and the beginning of homogeneous strain (HS). This mechanism avoids slip between layers and local concentrations of strain or area change. Homogeneous fold flattening (HF) at the end of folding increases the fold aspect ratio and decreases the ratio between the limb and the hinge thickness. Homogeneous strain superposed in the late stage of folding is not coaxial in many cases, with simple shear playing an important role, and gives rise to asymmetrical folds.

From the analysis of natural chevron folds and modelling with 'FoldModeler', we can consider that a common sequence that gives rise to chevron folds is LS-ETLS-PTLS-FF-HS. Homogeneous deformation mechanisms at the beginning and end of folding may be lacking, but the other three stages seem to be essential, although PTLS and FF can also operate simultaneously. Analysis of individual natural chevron folds, complemented with the use of 'FoldModeler', can be used to shed light on the particular sequences of folding mechanisms operating in those folds.

An inconsistency between strain measurements in natural chevron folds and strains obtained in theoretically modelled chevron folds has been found. Strains obtained by the Fry method in samples of the hinge zone and the limb are too low to be explained by theoretical modelling. Similar strain values have been measured by other authors in natural chevron folds (e.g. Yang and Gray, 1994). A possible explanation for this inconsistency is the operation of strain mechanisms that cannot be detected by centre-to-centre methods. In addition to brittle deformation, the more apparent deformation mechanism in the chevron folds analysed is pressure solution; nevertheless, grain-boundary sliding or grain sliding along anastomosing solution seams could have operated in association with pressure solution. These mechanisms are difficult to detect; Narahara and Wiltschko (1986) have also suggested, in addition to brittle deformation, undetectable grain-boundary sliding to explain the strain in a natural chevron fold.

In the context of the multilayer, field observation and geometrical modelling of chevron folds indicate that slip along the layers or simple shear parallel to bedding in incompetent layers is necessary for the development of this type of fold. Displacements involved must be maximum for tangential longitudinal strain mechanisms and minimum for flexural flow. Combinations of these mechanisms must give rise to situations between these extreme cases.

Acknowledgements

The present work was supported by Spanish CGL2005-02233-BTE project funded by Ministerio de Educación y Ciencia and Fondo Europeo de Desarrollo Regional (FEDER). We are grateful to two anonymous reviewers for many valuable suggestions that notably improved the manuscript, and to English Heritage for permission to collect rock samples in the Millook Haven area.

References

Aller, J., Bastida, F., Toimil, N.C., Bobillo-Ares, N.C., 2004. The use of conic sections for the geometrical analysis of folded surface profiles. Tectonophysics 379, 239–254.

Bastida, F., Bobillo-Ares, N.C., Aller, J., Toimil, N.C., 2003. Analysis of folding by superposition of strain patterns. Journal of Structural Geology 25, 1121–1139.

Bayly, M.B., 1964. A theory of similar folding in viscous materials. American Journal of Science 262, 753–766.

Bayly, M.B., 1976. Development of chevron folds: Discussion. Geological Society of America Bulletin 87, 1664.

Biot, M.A., 1961. Theory of folding of stratified viscoelastic media and its implications in tectonics and orogenesis. Geological Society America Bulletin 72, 1595–1620.

Biot, M.A., 1965. Mechanics of the Incremental Deformations. Wiley, New York, 504 pp.

Biot, M.A., Odé, H., Roever, W.L., 1961. Experimental verification of the theory of folding of stratified viscoelastic media. Geological Society of America Bulletin 72, 1621–1630.

Bobillo-Ares, N.C., Bastida, F., Aller, J., 2000. On tangential longitudinal strain folding. Tectonophysics 319, 53–68.

Bobillo-Ares, N.C., Toimil, N.C., Aller, J., Bastida, F., 2004. 'FoldModeler': a tool for the geometrical and kinematical analysis of folds. Computers & Geosciences 30, 147–159.

Bobillo-Ares, N.C., Aller, J., Bastida, F., Lisle, R.J., Toimil, N.C., 2006. The problem of area change in tangential longitudinal strain folding. Journal of Structural Geology 28, 1835–1848.

Carreras, J., Druguet, E., Griera, A., 2005. Shear zone-related folds. Journal of Structural Geology 27, 1229–1251.

Casey, M., Huggenberger, P., 1985. Numerical modeling of finite-amplitude similar folds developing under general deformation histories. Journal of Structural Geology 7, 103–114.

Chapple, W.M., 1968. A mathematical theory of finite-amplitude rock-folding. Geological Society of America Bulletin 79, 47–68.

Chapple, W.M., 1969. Fold shape and rheology: the folding of an isolated viscous-plastic layer. Tectonophysics 7, 97–116.

Chapple, W.M., 1970. The finite-amplitude instability in the folding of layered rocks. Canadian Journal of Earth Sciences 7, 457–466.

Currie, J.B., Patnode, H.W., Trump, R.P., 1962. Development of folds in sedimentary strata. Geological Society of America Bulletin 73, 665–674.

de Sitter, L.U., 1956. Structural Geology. McGraw-Hill, London.

de Sitter, L.U., 1958. Boudins and parasitic folds in relation to cleavage and folding. Geologie en Mijnbouw 8, 277–286.

Dieterich, J.H., 1970. Computer experiments on mechanics of finite amplitude folds. Canadian Journal of Earth Sciences 7, 467–476.

Dieterich, J.H., Carter, N.L., 1969. Stress-history of folding. American Journal of Science 267, 129–154.

Dubey, A.K., Cobbold, P.R., 1977. Noncylindrical flexural slip folds in nature and experiment. Tectonophysics 38, 223–239.

Ez, V., 2000. When shearing is a cause of folding. Earth-Science Reviews 51, 155–172.

Fletcher, R.C., Pollard, D.D., 1999. Can we understand structural and tectonic processes and their products without appeal to complete mechanics? Journal of Structural Geology 21, 1071–1088.

Fowler, T.J., Winsor, C.N., 1996. Evolution of chevron folds by profile shape changes: comparison between multilayer deformation experiments and folds of the Bendigo-Castlemaine goldfields, Australia. Tectonophysics 258, 125–150.

Fry, N., 1979. Density distribution techniques and strained length methods for determination of finite strains. Journal of Structural Geology 1, 221–229.

Ghosh, S.K., 1968. Experiments of buckling of multilayers which permit interlayer gliding. Tectonophysics 6, 207–249.

Hudleston, P.J., 1973. Fold morphology and some geometrical implications of theories of fold development. Tectonophysics 16, 1–46.

Hudleston, P.J., Srivastava, H.B., 1997. Strain and crystallographic fabric pattern in a folded calcite vein: the dependence on initial fabric. In: Sengupta, S. (Ed.), Evolution of Geological Structures in Micro- to Macro-Scales. Chapman & Hall, London, pp. 259–271.

Hudleston, P.J., Stephansson, O., 1973. Layer shortening and fold-shape development in the buckling of single layers. Tectonophysics 17, 299–321.

Hudleston, P.J., Treagus, S.H., Lan, L., 1996. Flexural flow folding: does it occur in nature? Geology 24, 203–206.

Johnson, A.M., 1970. Physical Processes in Geology. Freeman, Cooper & Co., San Francisco.

Johnson, A.M., Ellen, S.D., 1974. Theory of concentric, kink and sinusoidal folding. I. Introduction. Tectonophysics 21, 301–339.

Johnson, A.M., Fletcher, R.C., 1994. Folding of Viscous Layers: Mechanical Analysis and Interpretation of Structures in Deformed Rock. Columbia University Press, New York.

Johnson, A.M., Honea, E., 1975. A theory of concentric, kink, and sinusoidal folding and of monoclinal flexuring of compressible, elastic multilayers. Part III, transition from sinusoidal to concentric-like to chevron folds. Tectonophysics 27, 1–38.

Johnson, A.M., Pfaff, V.J., 1989. Parallel, similar and constrained folds. Engineering Geology 27, 115–180.

Kuenen, P.U., de Sitter, L.U., 1938. Experimental investigation into the mechanism of folding. Leidse Geologische Mededelingen 10, 217–240.

Lan, L., Hudleston, P.J., 1996. Rock rheology and sharpness of folds in single layers. Journal of Structural Geology 18, 925–931.

Narahara, D.K., Wiltschko, D.V., 1986. Deformation in the hinge region of a chevron fold, Valley and Ridge Province, central Pennsylvania. Journal of Structural Geology 8, 157–168.

Pfaff, V.J., Johnson, A.J., 1989. Opposite senses of fold asymmetry. Engineering Geology 27, 3–38.

Pollard, D.D., Fletcher, R.C., 2005. Fundamentals of Structural Geology. Cambridge University Press, Cambridge.

Ramberg, H., 1960. Relationship between length of arc and thickness of ptygmatically folded veins. American Journal of Science 258, 36–46.

Ramberg, H., 1963. Strain distribution and geometry of folds. Bulletin of the Geological Institute of Uppsala 42, 1–20.

Ramberg, H., 1964. Selective buckling of composite layers with contrasted rheological properties. A theory for simultaneous formation of several orders of folds. Tectonophysics 1, 307–341.

Ramberg, I.B., Johnson, A.M., 1976. Asymmetric folding in interbedded chert and shale of the Franciscan Complex, San Francisco Bay area, California. Tectonophysics 32, 295–320.

Ramsay, J.G., 1967. Folding and Fracturing of Rocks. McGraw-Hill, New York.

Ramsay, J.G., 1974. Development of chevron folds. Geological Society of America Bulletin 85, 1741–1754.

Ramsay, J.G., Huber, M.I., 1987. Modern Structural Geology, Vol. 2. Folds and Fractures. Academic Press, London.

Smythe, D.K., 1971. Viscous theory of angular folding by flexural flow. Tectonophysics 12, 415–430.

Stewart, K.G., Alvarez, W., 1991. Mobile hinge kinking in layered rocks and models. Journal of Structural Geology 13, 243–259.

Tanner, P.W.G., 1989. The flexural-slip mechanism. Journal of Structural Geology 11, 635–656.

Yang, X., Gray, D.R., 1994. Strain, cleavage and microstructure variations in sandstone: implications for stiff layer behaviour in chevron folding. Journal of Structural Geology 16, 1353–1365.